MnS AND CdS CLUSTERS ENCAPSULATED IN NATURAL ZEOLITES

F. Iacomi

Department of Physics, "Al. I. Cuza" University, R-6600, Iasi, Romania

MnS and CdS clusters were synthesized inside some natural zeolite frameworks by treating the Mn^{2+}, Cd^{2+} ion exchanged forms with 1 molar aqueous solution Na_2S. The optical and EPR spectra suggest that semiconductor clusters are formed into the zeolite channels. The absorption edge changes as a function of cluster-cluster contact distance in the zeolite (from 475 nm, for clinoptilolite-CdS, to 350 nm, for laumontite-CdS). The crystalline fields of exchange sites determines the manganese species and the nature of MnS clusters ($E_g = 3.1 – 4.66$ eV). The formation of semiconductor clusters into zeolites modifies the zeolite electrical properties.

1. Introduction

Recent advances in semiconductor cluster synthesis have opened the door towards systematic studies of small clusters in the condensed phase. Clusters with diameters ranging from 10 to 150 Å can be synthesized in a variety of media such as polymers, glasses, zeolites [1,2]. Size dependence of their optical, electronic and possibly other properties dictates that the censsers exhibit a narrow distribution of their average diameters.

The zeolite structures allow to vary the cluster concentration, and the intercluster geometry in a controlled manner over the periodicity defined by the host zeolite lattice [3,4]. Host matrices like zeolites reduce the interchain and interlayer perturbation often encountered in other low dimensional solids [5].

In this work we report our observations of small MnS and CdS clusters formed inside the channels of two natural zeolite frameworks: microcrystalline clinoptilolite and laumontite single crystal. Clinoptilolite is one of the most abundant natural zeolite and has a broad spectrum of industrial applications. The clinoptilolite structure exhibits three types of structural channels confined by tetrahedral ring systems. A and B channels run paralel to c–axis and are confined by ten- and eight-membered rings of tetrahedra with a highly dezordered Si, Al distribution(7.05×4.25 Å respectively 4.60×3.95 Å). C channels which are determined by another set of eight- membered rings run paralel to *a* axis and the [102] direction. The channel system is two-dimensional parallel to (010). Exchange cations (Na, K, Ca, Mg) exhibit a coordination to framework oxygens and water molecules in the channels [6,7]. Laumontite, a less common zeolite, is a monoclinic mineral characterized by single 4 – ring tetrahedral chains as secondary building units and large channels of ten - membered tetrahedral rings (4.6×6.4 Å) which are parallel to *c*-axis. The channels are occupied by Ca and H_2O and minor Na and K [8,9].

The optical and electrical properties of semiconductor clusters in zeolites were investigated.

2. Experimental

The semiconductor clusters were prepared in water media, according to the procedure of Barnakov et al. [10], who noted that the stability of the samples obtained by this mehod is very high. In order to remove the impurities, the powdered clinoptilolite, from Mârsid-Romania, was first submited to an acid treatement, using 1N HCl solutions [11]. The zeolites in their sodium cation form were first thermally treated at 673K during 4 h and then ion-exchanged by treating with 0.1 N aqueous cadmium (pH = 5.5) or manganese nitrate solutions at 296K (pH= 5.8), using a solid/liquid ratio of 1/50. The ion loaded zeolites, were washed and dried at 378 K and then submitted to a sulfidation process with 1M Na_2S solution, at room temperature, during 12 h (S/L=1/50). In such a

process CdS and MnS clusters precipitate in the zeolite framework and Na-form of zeolite was regenerated. The atomic absorption method evidenced a S/Cd ratio of 3.51 and a S/Mn ratio of 1.1.

X-ray powder diffraction patterns for these materials showed that zeolite crystallinity was maintained during synthesis. Most notable was that no peaks for the bulk semiconductor phase were evident in the powder data

The optical absorption spectra at 300 K were obtained using a SPECORD UV/VIS spectrophotometer in the wavelength range 300-800 nm. Luminiscence spectra were also obtained at room and liquid-nitrogen temperature with pulsed excitation (λ=337.1 nm, ν=72 Hz, τ=10^{-8}s, 1.6 kW). EPR measurements were performed at room temperature with a RADIOPAN spectrometer in X band.

Measurements of the electric resistance as a function of temperature were made in air, in the range of 293 - 794 K, by means of an experimental set-up using a KEITHLEY 6517A instrument. Pellets of 7mm diameter and 1mm thick were prepared by pressing the powdered samples at 10 tf/cm^2.

3. Results and Discussion

3.1. Optical absorption

The optical absorption spectra give the quantization effect as the estimation of band gap(Fig.1). It is evident that discrete CdS clusters interconnect electronically by quantum tunneling forming a semiconductor supercluster with behavior intermediate between that of discrete clusters and bulk semiconductor(E_g=2.76 eV, E_g = 3.55 eV). This suggests that using two types of zeolites as template can be built with the same (CdS)$_4$ building block two types of superclusters [12]. The data showed an orientational effect on the optical properties of CdS superclusters. The absorption edge changes as a function of cluster-cluster contact distance in the zeolite(from 450 nm, for CLI-CdS, to 350 nm, for LAU-CdS). Because strong coupling with the host lattice occures through the interaction between Cd and framework oxygen, the phonon broadening becomes important. The partial occupancy of zeolite sites by Cd^{2+} produces CdS supercluster size distributions in the zeolite lattice rather than the more desirable homogeneous semiconductor superlattice.
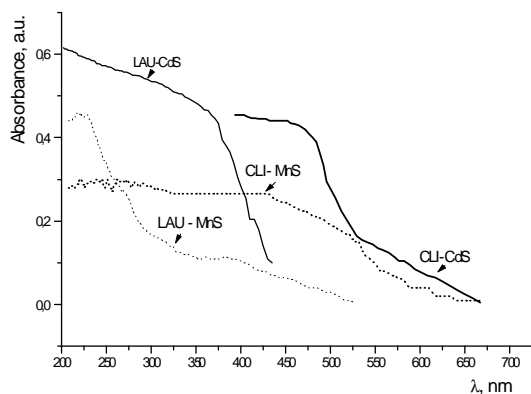

Fig. 1. Absorption spectra of MnS and CdS clusters in natural zeolites.

These are the first experimental data on MnS clusters encapsulated in zeolites. The S-S and Mn-Mn distances and atomic charges are responsible for the bandwidths [13]. Tappero and Lichanot investigated the geometry and electronic structure of bulk α-MnS. The band structures and their associated densities of states indicated a large hybridization between the sulfur p and manganese d orbitals. The value of the gap was closed to 1.5 eV and was understimated by 1.2 eV as regarding the experimental value of Sato et al. [14]. The β band structure (bandwith =3.81 eV) was ascribed to the 0.44 e charge transfer from S^{2-} to Mn^{2+} with respect to ideal ionic configuration. The optical spectrum of MnS-LAU shows three partially resolved quantum excitonic peaks (387 nm, 309 nm. 266 nm) while the MnS – CLI shows a plateau in the 318 – 427 nm region and an excitonic peak at 530 nm.

3.2. Photoluminiscence

Photoluminiscence of semiconductor clusters provide different energy states available between valence band and conduction band responsible for radiative recombination.

The room-temperature spectra of CdS doped zeolites are characterized by broad-band emission consisting of two main bands (Fig.2, tab.1)[15].
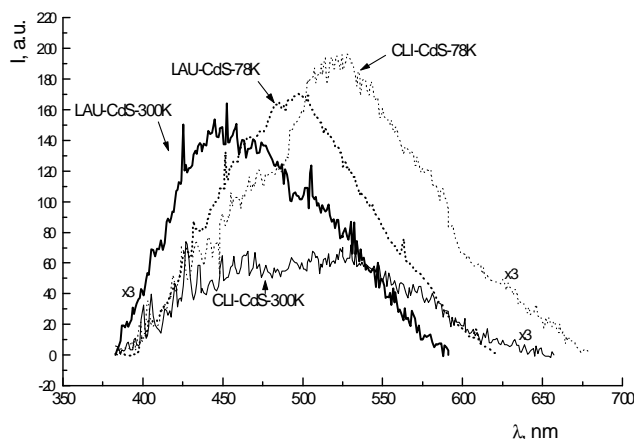

Fig. 2. Room-and low temperature emission spectra of CdS in natural zeolites .

For monodisperse particles with highly symmetric shapes, there exists sharp resonances in the optical region, corresponding to the natural modes of oscillation of the structure. When the wavelength approaches to the absorption edge, the local field intensity at the surface increases for small clusters and decreases for large particles. This is due to the sensitivity of the structural resonance peaks to the absorption. It is important to realize that although these sharp resonance peaks cannot be observed for an ensemble of particles with broad size distribution [16]. The local field effect is shown to be substantial for semiconductor clusters encapsulated in clinoptilolite. In order to investigate the main photoluminescence bands a background correction was carried out by a spline fit, and the corrected spectrum was deconvoluted into Gaussian components. The results are shown in Table 1.
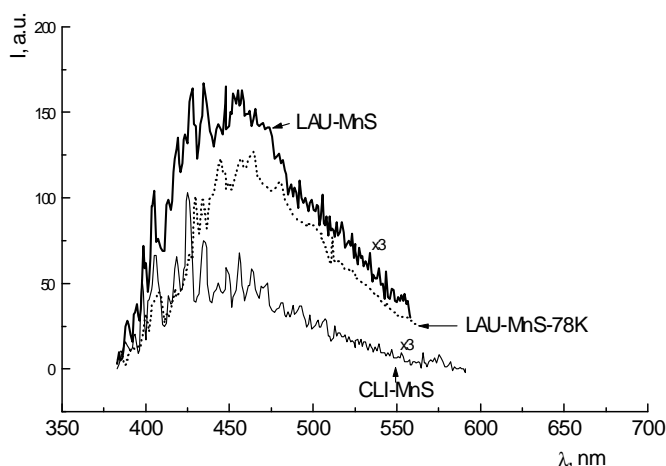

Fig. 3. Room- and low-temperature emission spectra of MnS in natural zeolites.

Table 1. The main emission bands of photoluminiscence spectra.

Sample	Emission bands at 300K, nm	Emission bands at 78K	Sample	Emission bands at 300K, nm	Emission bands at 78K, nm
CLI-CdS	444 520	442 520 623	CLI-MnS	422 467	422 467
LAU-CdS	439 499	441 495	LAU-MnS	426 460 513	451 524

As the temperature is lowered, the emission intensity increases and the emission peak shifts to lower energies (Figs. 2, 3). The emisssion spectra revealed major peaks at 440, 500, 520 and 623 nm. The 440 nm emission was also observed in zeolite A, and attributed to sulfur related defect. The emission peaking at ~500 nm is consistent with the dominance of fluorescence by transition coupling from the extended to the localized states. The localized states are presumable very closely spaced near the edge of the valunce band and are populated by holes without a pump due to thermal activation. The higher energy emission peaking at ca 520 nm is consistent with an interaction of Lewis center with cadmium vacancies. The band at 623 nm observed at 78 K for CLI-CdS (Fig. 2) corresponds to the deep trap emission [17]. This band was also observed for CdS nanocrystallites stabilized by DNA and was attributed to cadmium atom defect sites in the cluster [18].

MnS clusters have 1:1 manganese–to-sulfur ratios and yield weakly emissive samples (Fig. 3). The blue band at 460 nm is atributed to the donor-acceptor pair transition in which the acceptor is related to the Mn^{2+} vacancy. Such vacancies should be compensated by the predominantly present Na^+ in the zeolite channels or by the formation of $S^-(S^{2+}+$ hole). The band at 510-520 nm was observed only in laumontite and its origin is still unknown. The red shift of MnS emission spectra, at 78 K, is negligible, suggesting a stronger interaction with the zeolite lattice and a better stability.
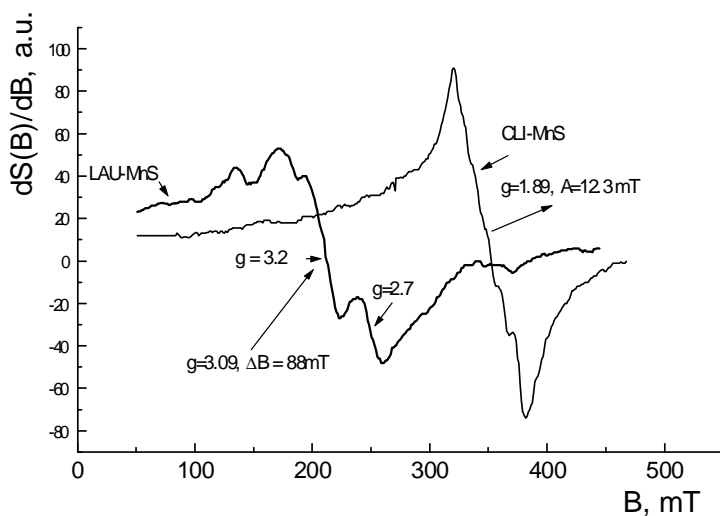

Fig. 4. Room temperature EPR spectra of LAU-MnS and CLI-MnS.

3.3. EPR

The EPR experiments clear evidence major differences in Mn species encapsulated in laumontite and clinoptilolite (Fig. 4). The EPR spectrum of CLI-MnS consist of a hyperfine sextet spectrum superposed on a broad background centered at about g = 1.89 (ΔB = 62 mT, A=12.3 mT, ΔB = 140 mT). The unequal signal intensities of the hyperfine sextet demonstrate that the symmetry of Mn ions is lower than cubic phase. It is clear that at least a fraction of these sites are characterized by crystal field effects small enough to be treated as perturbations. The second is the broad background that is attributed to strong dipole-dipole interaction between Mn ions in clusters. The EPR spectrum of Mn-CLI evidenced only the hiperfine sextet at g = 1.89, A = 8.7 mT, characteristic for isolated Mn^{2+} ions in exchange positions. The MnS cluster formation determined modifications in the A value and in the intensity of hyperfine sextet spectrum and the appearance of the broad spectrum. The broad EPR spectrum can be related to the absorption peak at 530 nm (E_g = 2.34 eV).

The MnS cluster formation in the laumontite channels affects only the linewidth of the EPR signal, which becomes larger (Fig. 4). In laumontite channels, Mn ions form polimeric species which gives EPR signals at low magnetic fields. Three of them, characterized by g = 2.7, g = 3.0 and g = 3.2 contribute to the three excitonic peaks located at 266 nm, 387 nm and 309 nm.

3.4. The electrical conductivity

The electrical conductivity of zeolites in their cation forms and with semiconductor clusters was studied as a function of temperature (Fig. 5). The formation of semiconductor clusters into the zeolite channels determines the increase in electrical conductivity and the sharp decrease in the activation energy of electrical conductivity, ΔE (Table 2).
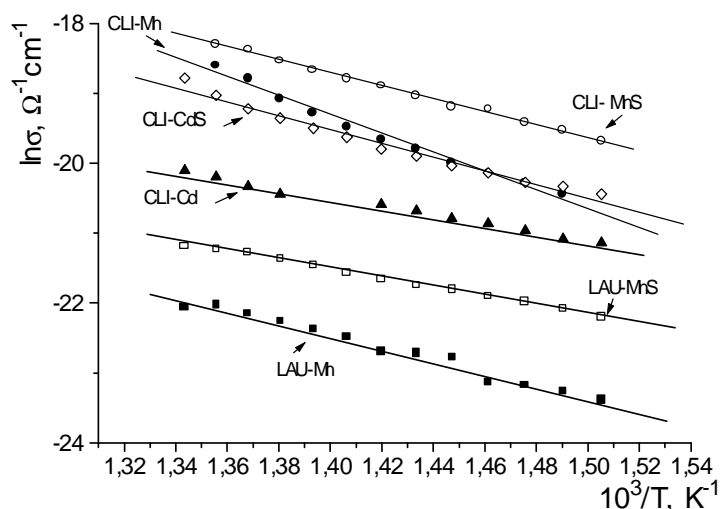

Fig. 7. The dependence of electrical conductivity of natural zeolites on the temperature and on the zeolite form.

Table 2. The values of the activation energy of electrical conductivity.

Sample	CLI-Mn	CLI-MnS	LAU-Mn	LAU-MnS	CLI-Cd	CLI-CdS
ΔE, eV	2.35	1.60	1.55	1.10	1.07	1.70

The differences in ΔE values, calculated from the dependence $\sigma = f(10^3/T)$, can be related to the substitutional or interstitial Na impurities. The changes in electrical properties are due to systematic transformations in the density of electronic energy levels as a function of the size, known as quantum size effects.

4. Conclusions

Well-defined CdS and MnS clusters and superclusters have been synthesised within the pore structure of natural zeolites climoptilolide and laumontite.

The ion-exchange method cannot fill up the zeolite channels, and disorder exists. The vacancies and imperfections break up the supercluster and introduce in homogeneities in the supercluster size distribution, which is the reason for the broad exciton absorption peak. For very small clusters the lattice structures and orbital hybridization may change in order to minimize surface dangling bonds and maximize bulk bonding. The appearance of the emission spectra specific to intrinsec defects of a well defined aggregate structure marks the onset of semiconductor properties. Phenomena such as trapping are connected with electronic states at the zeolite-semiconductor

interface. The MnS cluster formation into the zeolite channels was suported by optical and EPR spectra. Quantum confinement leads to changes in g factors, HFS constants and linewidths.

There is a strong dependence of the electrical conductivity on the dimensions of zeolite channels, and on local fields at the surface of the semiconductor clusters.

References

[1] Y. Wang, W. Mahler, Opt. Commun., **61**, 233 (1987).

[2] E. Helinski, P. Lucas, Y. Wang, J. Chem. Phys, **89**, 3435 (1988)

[3] G. B. Banfi, V. Degiorgio, D. Ricard, Adv. Phys., **47**, 447 (1998).

[4] J. Brus, J. Phys. Chem. **90**, 2555 (1986).

[5] O. Terasaki, K. Yamazuki, J. M. Thomas, T. Ohsuna, D. Watanabe, J. V. Sanders, J. C. Barry, Nature, **58**, 330 (1987).

[6] K. Koyama, Y. Takeuchi, Z. Kristallogr. **145**, 216 (1977).

[7] F. Iacomi, E. Popovici, M. Alexandroaei, A. Barbat, An. St. Univ. "Al. I. Cuza" Iasi, **XXXII**, sIb, Fizica 99 (1986).

[8] D. W. Ming, F. A. Mumpton, Natural Zeolites '93, Occ. Prop. Use, New York (1995).

[9] I. Bedelean, S. D. Stoici, Zeoliti Naturali, Ed. Tehn., Bucuresti (1984).

[10] Yu. A. Barbnakov, M. S. Ivanova, V. P. Petranovskii, V. V. Poborchii, V. G. Soloviev, A. F. Ioffe, S. M. Kirov, Zeolites and Related Microporous Materials: State of the Art 1994, Studies in Surface Science and Catalysis, vol. 84, Eds. J. Weitkamp, H. G. Karge, H. Pfeifer, W. Holde-rich, Elsevier Science B. V. 575 (1994).

[11] E. Popovici, F. Iacomi, G. Singurel, E. Trif, Al. Nicula, Anal. Letters, **21(10)**, 1901 (1988).

[12] N. Herron, Y. Wang, M. M. Eddy, G. D. Stucky, D. E. Cox, K. Moller, T. Bein, J. Am. Chem. Soc., **111**, 530 (1989).

[13] R. Tappero, A. Lichanot, Chem. Phys.**236**, 97 (1998).

[14] H. Sato, T. Mihara, A. Furuta, Y. Ueda, H. Namatame, M. Taniguchi, J. Elect. Spect. And Related Phenomena, **78**, 87 (1996).

[15] Y. Wang, N. Herron, J. Phys. Chem. 95, 52 5(1991).

[16] Y. Wang, J. Phys. Chem., **95**, 119 (1991)

[17] Y. Wang, N. Herron, J. Phys.Chem, **92**, 4988 (1988).

[18] J. L. Coffer, S. R. Bigham, R. F. Pinizzotto, H. Yang, Nanotechnology, **3**, 69 (1992).